Available online at www.sciencedirect.com

SCIENCE DIRECT

Developmental Biology 278 (2005) 367–380

DEVELOPMENTAL BIOLOGY

www.elsevier.com/locate/ydbio

A maternal store of macroH2A is removed from pronuclei prior to onset of somatic macroH2A expression in preimplantation embryos

Ching-Chien Chang[a,b], Yinghong Ma[a], Stephanie Jacobs[a], X. Cindy Tian[a,b], Xiangzhong Yang[a,b], Theodore P. Rasmussen[a,b,c,*]

[a]*Center for Regenerative Biology, University of Connecticut, 1392 Storrs Road, Storrs, CT 06269-4243, USA*
[b]*Department of Animal Science, University of Connecticut, Storrs, CT 06269-4040, USA*
[c]*Department of Molecular and Cell Biology, University of Connecticut, Storrs, CT 06269-3042, USA*

Received for publication 24 May 2004, revised 1 November 2004, accepted 11 November 2004
Available online 19 December 2004

Abstract

MacroH2A histones are variants of canonical histone H2A that are conserved among vertebrates. Previous studies have implicated macroH2As in epigenetic gene-silencing events including X chromosome inactivation. Here we show that macroH2A is present in developing and mature mouse oocytes. MacroH2A is localized to chromatin of germinal vesicles (GV) in both late growth stage (lg-GV) and fully grown (fg-GV) stage oocytes. In addition, macroH2A is associated with the chromosomes of mature oocytes, and abundant macroH2A is present in the first polar body. However, maternal macroH2A is lost from zygotes generated by normal fertilization by the late 2 pronuclei (2PN) stage. Normal embryos at 2-, 4-, and 8-cell stages lack macroH2A except in residual polar bodies. MacroH2A protein expression reappears in embryos after the 8-cell stage and persists in morulae and blastocysts, where nuclear macroH2A is present in both the trophectodermal and inner cell mass cells. We followed the loss of macroH2A from pronuclei in parthenogenetic embryos generated by oocyte activation. Abundant macroH2A is present upon the metaphase II plate and persists through parthenogenetic anaphase, but macroH2A is progressively lost during pronuclear decondensation prior to synkaryogamy. Examination of embryos generated by intracytoplasmic sperm injection (ICSI) revealed that macroH2A is associated exclusively with female pronuclei prior to loss in late pronucleus stage embryos. These results outline a surprising finding that a maternal store of macroH2A is removed from the maternal genome prior to synkaryogamy, resulting in embryos that execute three to four mitotic divisions in the absence of macroH2A prior to the onset of embryonic macroH2A expression.

Keywords: MacroH2A; Histone; Oocyte; Germinal vesicle; Epigenetic; Preimplantation; Parthenogenesis

Introduction

Gametogenesis yields haploid eggs or sperm whose DNA is packaged within specialized chromatin that differs markedly between the sexes. Shortly after fertilization, maternal and paternal genomes and their associated chromatin commence a series of broad and rapid reorganizations during the ensuing period of preimplantation development. These chromatin dynamics are of special interest because chromatin is the principle molecular basis for epigenetic regulation of gene expression. Therefore, studies of gametic chromatin and its subsequent reorganization in the preimplantation embryo promise to shed light on processes such as imprinting, reprogramming associated with somatic cell nuclear transfer, and developmentally regulated gene expression.

In developing and mature oocytes, the maternal genome is packaged within nucleosomes that contain a high content of the oocyte-specific histone variant H1FOO (H1oo) (Tanaka et al., 2001). The maternal genome of mature oocytes contains histones that lack appreciable levels of

* Corresponding author. Center for Regenerative Biology. University of Connecticut, Advanced Technology Laboratory, 1392 Storrs Road, Storrs, CT 06269-4243, USA. Fax: +1 860 486 8809.
E-mail address: theodore.rasmussen@uconn.edu (T.P. Rasmussen).

0012-1606/$ - see front matter © 2004 Elsevier Inc. All rights reserved.
doi:10.1016/j.ydbio.2004.11.032

acetylation (Kim et al., 2003). In addition, the maternal genome in MII oocytes contains histone H3 that is modified by methylation at lysine 9 (Arney et al., 2002; Liu et al., 2004). Thus, mature oocytes contain chromatin in a state that is generally nonpermissive for transcription. The paternal genome in sperm is packaged in a highly condensed and transcriptionally inert configuration in which the vast majority of histones have been replaced with protamines, assembled upon DNA that is highly methylated upon CpG dinucleotides.

In mice, male and female genomes undergo broad and rapid chromatin reorganizations shortly after fertilization leading to zygotic genome activation at the late 2 pronucleus (2PN) stage of single-cell embryos (Ram and Schultz, 1993). The male pronucleus is rapidly stripped of protamines, undergoes significant decondensation, and histones of maternal origin (including H1FOO) are assembled upon the paternal genome (Gao et al., 2004; Teranishi et al., 2004). In addition, male pronuclear decondensation is associated with active demethylation of CpG dinucleotides of DNA to levels similar to that of the female pronucleus (Mayer et al., 2000; Oswald et al., 2000). The maternal genome behaves quite differently: The maternal genome is arrested at metaphase II (MII) in mature oocytes. Upon fertilization, chromosomes present at the oocyte metaphase plate migrate to separate poles, and a haploid set of maternal chromosomes are extruded as the second polar body. Prior to synkaryogamy, male and female pronuclei individually execute a single S-phase, merge, and rapidly complete the first embryonic mitosis.

Subsequent stages of preimplantation development are characterized by progressive, coordinated remodeling of embryonic chromatin. In mice, histones become acetylated at the late 2 pronuclei (2PN) stage (Kim et al., 2003), a timing that is roughly coincident with zygotic genome activation. Histone H1FOO is removed at the 2-cell stage and the embryonic genome does not acquire somatic linker histone H1 until the 4-cell stage (Gao et al., 2004). A second wave of preimplantation embryonic gene activation occurs as morulae develop to blastocysts (Hamatani et al., 2004).

The histone variant macroH2A is a core histone related to canonical H2A that possesses a lengthy C-terminal nonhistone domain (NHD) (Pehrson and Fried, 1992). A number of studies suggest a general involvement of macroH2A in heterochromatin: MacroH2A associates with the facultative heterochromatin of inactive X chromosomes in female somatic cells (Costanzi and Pehrson, 1998). However, macroH2A1 is expressed at similar levels in male and

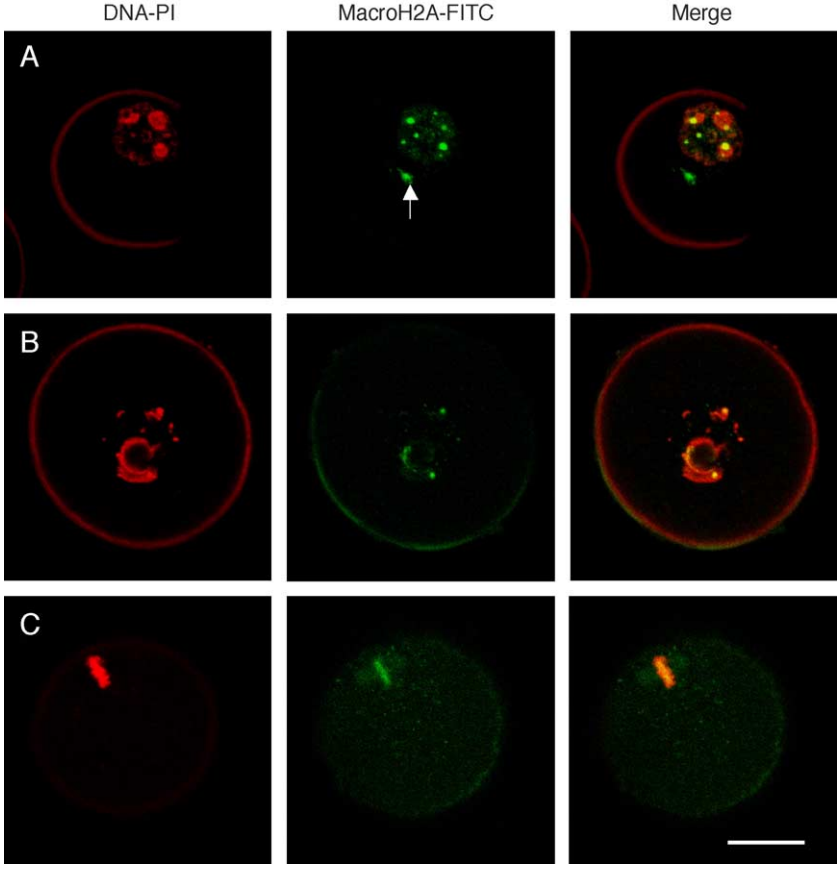

Fig. 1. Localization of histone macroH2A during oocyte maturation. Confocal images of individual maturing oocytes stained with propidium iodide to visualize the DNA (DNA-PI) combined with immunodetection with α-macroH2A antibody detected with FITC (macroH2A-FITC). (A) A representative oocyte at the late growth stage germinal vesicle stage (lg-GV). The arrow indicates an extranuclear, presumptive centrosomal concentration of macroH2A. (B) A representative oocyte at the fully grown GV stage (fg-GV). (C) A representative mature oocyte arrested at meiotic metaphase II (MII). Scale bar = 30 μm.

female cells (Rasmussen et al., 1999), suggesting that its function is not restricted to X chromosome inactivation. Additional analyses show that macroH2A can inhibit transcription because it can down-regulate NF-kappaB transcription factor binding and impedes SWI/SNF chromatin remodeling (Angelov et al., 2003). MacroH2A may also influence ADP-ribosylation of histones through a motif present in the macroH2A NHD (Ladurner, 2003). MacroH2A is widely expressed in blastocyst stage embryos, which contain detectable macroH2A present upon X chromosomes subject to imprinted inactivation in trophectodermal cells of female blastocysts (Costanzi et al., 2000). Additional studies show that macroH2A often resides in close proximity to pericentric heterochromatin (Costanzi et al., 2000), often in juxtaposition to heterochromatin protein 1β (Hoyer-Fender et al., 2004; Turner et al., 2001), a marker of pericentric heterochromatin.

MacroH2A has been analyzed extensively during murine spermatogenesis. MacroH2A is expressed during the pachytene stage of spermatogenesis, where it is associated with sex vesicles containing sequestered X and Y chromosomes (Hoyer-Fender et al., 2000, 2004; Richler et al., 2000), but unlike somatic cells, this association does not require Xist RNA (Turner et al., 2002). In addition, macroH2A has been shown to associate with pericentric chromatin of all chromosomes in pachytene oocytes (Hoyer-Fender et al., 2004). Here we show that macroH2A is retained during the remainder of oocyte maturation and is present in mature oocytes. Upon fertilization, a transient asymmetry exists in which macroH2A preferentially associates with the female pronucleus. This maternal store of macroH2A is removed by the late 2 pronuclei stage and macroH2A protein of embryonic origin does not appear until after the 8-cell stage. This finding shows that embryos complete their first three to four cell cycles in the absence of macroH2A, a pattern quite different than that observed for linker H1 histones. Together, these results suggest that the coordinated phases of embryonic genome activation are exquisitely coordinated with extensive chromatin remodeling of the early embryonic genome. These results show that dramatic alterations in the content of histone variants occur in the chromatin of developing preimplantation embryos.

Materials and methods

Chemicals

Unless otherwise indicated, all chemicals were purchased from Sigma (St. Louis, MO).

Animals and recovery of oocytes and embryos

CD-1 mice (Charles River Laboratories, Wilmington, MA, USA) were used to obtain MII unfertilized oocytes, sperm, and zygotes (12 h after mating). Female B6D2F1 mice (Charles River Laboratories) were used to obtain MII oocytes for intracytoplasmic sperm injection (ICSI). Oocytes at the germinal vesicle (GV) stage were retrieved from ovaries harvested from CD-1 mice aged 8–12 weeks. Follicles within ovaries were punctured with a sterile 25-gauge needle. After collection of granulosa oocyte complexes (GOC), oocytes

Table 1
Developmental distribution of macroH2A

Group	Developmental stage[a]	Time	Number examined	No. of oocytes/ embryos showing macroH2A signal in nucleus (%)
Oocyte maturation	lg-GV oocyte	N/A	13	13 (100)
	fg-GV oocyte	N/A	22	22 (100)
	MII oocyte	N/A	17	17 (100)
Preimplantation development	2PN	22 h[b]	12	0 (0)
	2-cell	48 h[b]	18	0 (0)
	4-cell	60 h[b]	18	0 (0)
	8-cell	70 h[b]	14	0 (0)
	9–12 cell[c]	70 h[b]	7	3 (42.8)
	Morula	84 h[b]	22	22 (100)
	Blastocyst	104 h[b]	22	22 (100)
Parthenogenetic activation	Act 10 min	10 min[d]	9	9 (100)
	Act 1 h	1 h[d]	8	8 (100)
	Act 3 h	3 h[d]	16	16 (100)
	Act 4.5 h	4.5 h[d,e]	5	5 (100)
	Act 6 h	6 h[d,e]	15	15 (100)
	Act 12 h	12 h[d,e]	10	0 (0)

[a] Abreviations: lg-GV: late growth stage germinal vesicle; fg-GV: fully grown germinal vesicle; MII: metaphase II; 2PN: 2 pronuclei.
[b] Hours after hCG injection.
[c] At the 70-h time-point, some embryos had undergone asynchronous cell divisions resulting in 9–12 nuclei.
[d] Time after oocyte activation.
[e] At these time points, a progressive loss of signal to undetectable levels of macroH2A after 12 h of parthenogenetic development was observed.

with diameters of less than 70 μm (associated with compact granulosa cells) were classified as late growth stage germinal vesicle (lg-GV) oocytes. Oocytes larger than 75 μm (associated with loosely attached granulosa cells) were classified as fully grown germinal vesicle (fg-GVs) oocytes. GOCs containing lg-GV oocytes were treated with 1.5 mg/ml collagenase at 37°C for 30 min, after which the granulosa cells were stripped by repeated aspiration through a glass pipette. Oocytes containing fg-GVs were stripped of granulosa cells by repeated aspiration of untreated GOCs through a glass pipette, the tip diameter of which was slightly larger than the diameter of an oocyte. The granulosa-denuded GV oocytes were then transferred into acidic Dulbecco's PBS (pH 2.5) to remove zona pellucida.

Mature MII stage oocytes were collected from female CD-1 mice subjected to the following hormone priming protocol: Superovulation was induced with 10 IU of equine chorionic gonadotrophin (eCG) followed 48 h later with 10 IU of human chorionic gonadotrophin (hCG). Oocytes were freed of cumulus cells by brief exposure to 300 IU/ml of hyaluronidase at 37°C and gentle pipetting. Denuded MII oocytes were either subjected to oocyte activation or prepared for immunofluorescence by removing the zona pellucida with acidic Dulbecco's PBS (pH 2.5), followed by

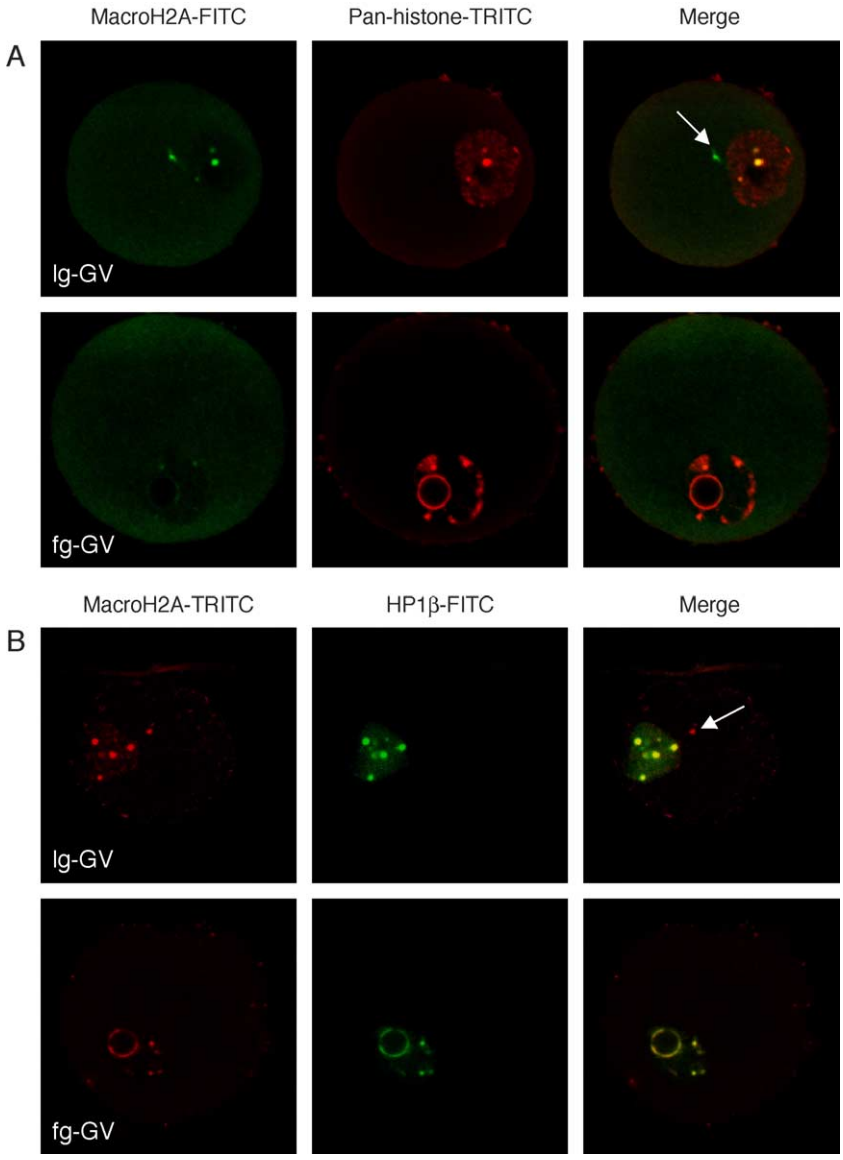

Fig. 2. Distribution of macroH2A relative to chromatin markers in lg-GV and fg-GV stage oocytes. (A) Mouse lg-GV and fg-GV stage oocytes were subjected to double immunofluorescence using antibodies against macroH2A (detected with FITC, green) and an antibody with general reactivity toward histones (pan-histone, detected with TRITC, red). Note that macroH2A protein is restricted to condensed chromatin in both stages. (B) Mouse lg-GV and fg-GV stage oocytes were subjected to immunofluorescence using the antibodies against macroH2A (detected with TRITC, red) and the heterochromatin component HP1β (detected with FITC, green). Note the extensive colocalization of macroH2A with HP1β. Arrows indicate extranuclear concentrations of macroH2A that likely coincide with centrosomes in lg-GV oocytes (see Fig. 3A).

fixation in 4% paraformaldehyde in PBS for 15 min at room temperature.

Female CD-1 mice, averaging 8 weeks of age, were superovulated to provide embryos as described (Hogan et al., 1994). After superovulation with 10 IU of eCG followed by 10 IU of hCG 48 h later, females were paired with CD-1 males and inspected the following morning for copulation plugs. Preimplantation embryos were flushed from oviducts after the hCG treatment and incubated in KSOM + AA medium (Specialty Media, Phillipsburg, NJ) before fixation. Specifically, pronuclear stage embryos (2PN) were harvested and fixed at 22 h, 2-cell embryos at 48 h, 4-cell embryos at 60 h, 8-cell and 9- to 12-cell embryos at 70 h, morulae embryos at 84 h, and blastocyst embryos at 104 h, after hCG injection.

Oocyte parthenogenetic activation

Mature MII oocytes were collected from CD-1 female mice at 15 h after hCG treatment, then subjected to parthenogenetic activation by exposure to activation medium (calcium-free KSOM, 10 mM strontium chloride, and 5 μg/ml cytochalasin B) for 6 h. Oocytes were fixed after 10 min, 1, 3, 4.5, 6, and 12 h after in activation medium.

Intracytoplasmic sperm injection

Male CD-1 mice, 12 weeks of age, were used to obtain sperm. The caudal epididymus was excised and then punctured with a 25-gauge needle several times to release

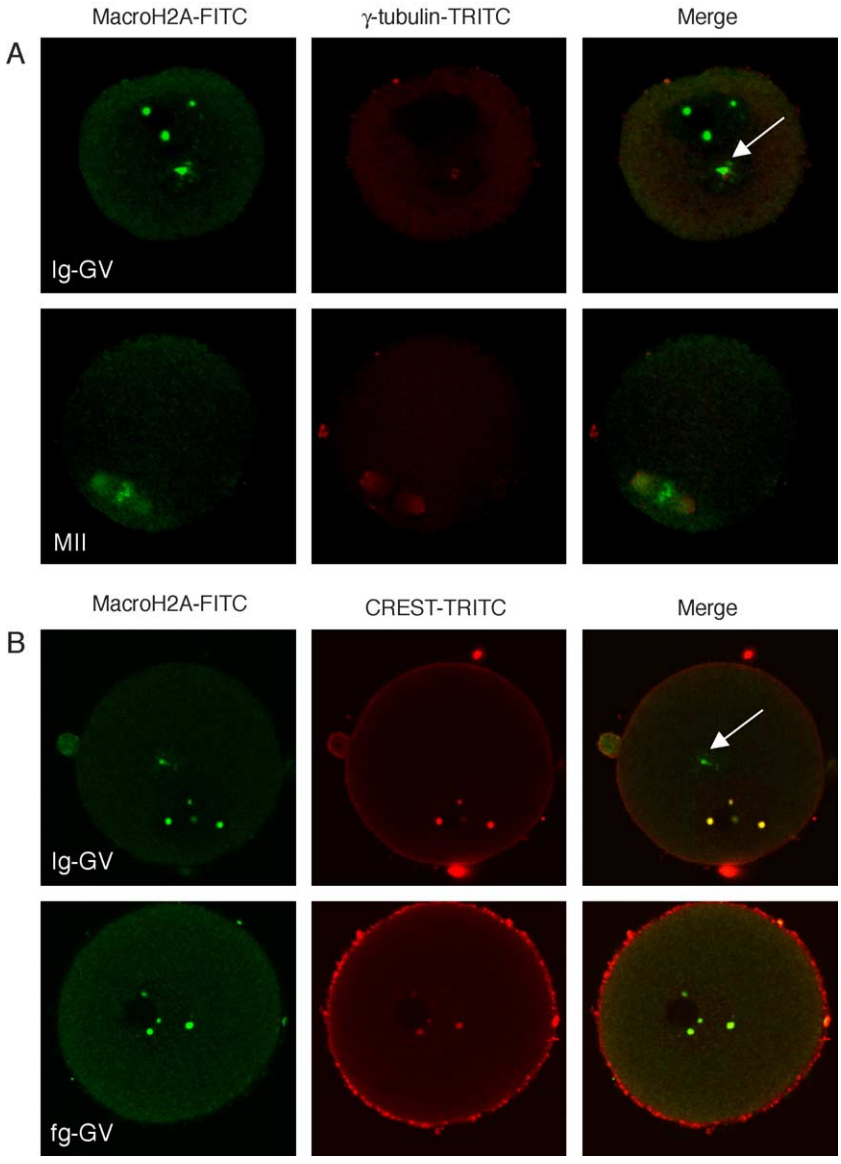

Fig. 3. Expression of macroH2A relative to centrosome (γ-tubulin) and centromere (CREST) proteins in developing oocytes. (A) Mouse lg-GV and MII oocytes were subjected to double immunofluorescence with antibodies against macroH2A (detected with FITC, green) and γ-tubulin (detected with TRITC, red). (B) Mouse lg-GV and fg-GV oocytes were subjected to double immunofluorescence with antibodies against macroH2A (detected with FITC, green) and CREST antisera (detected with TRITC, red). Arrows indicate extranuclear, centrosomal concentrations of macroH2A.

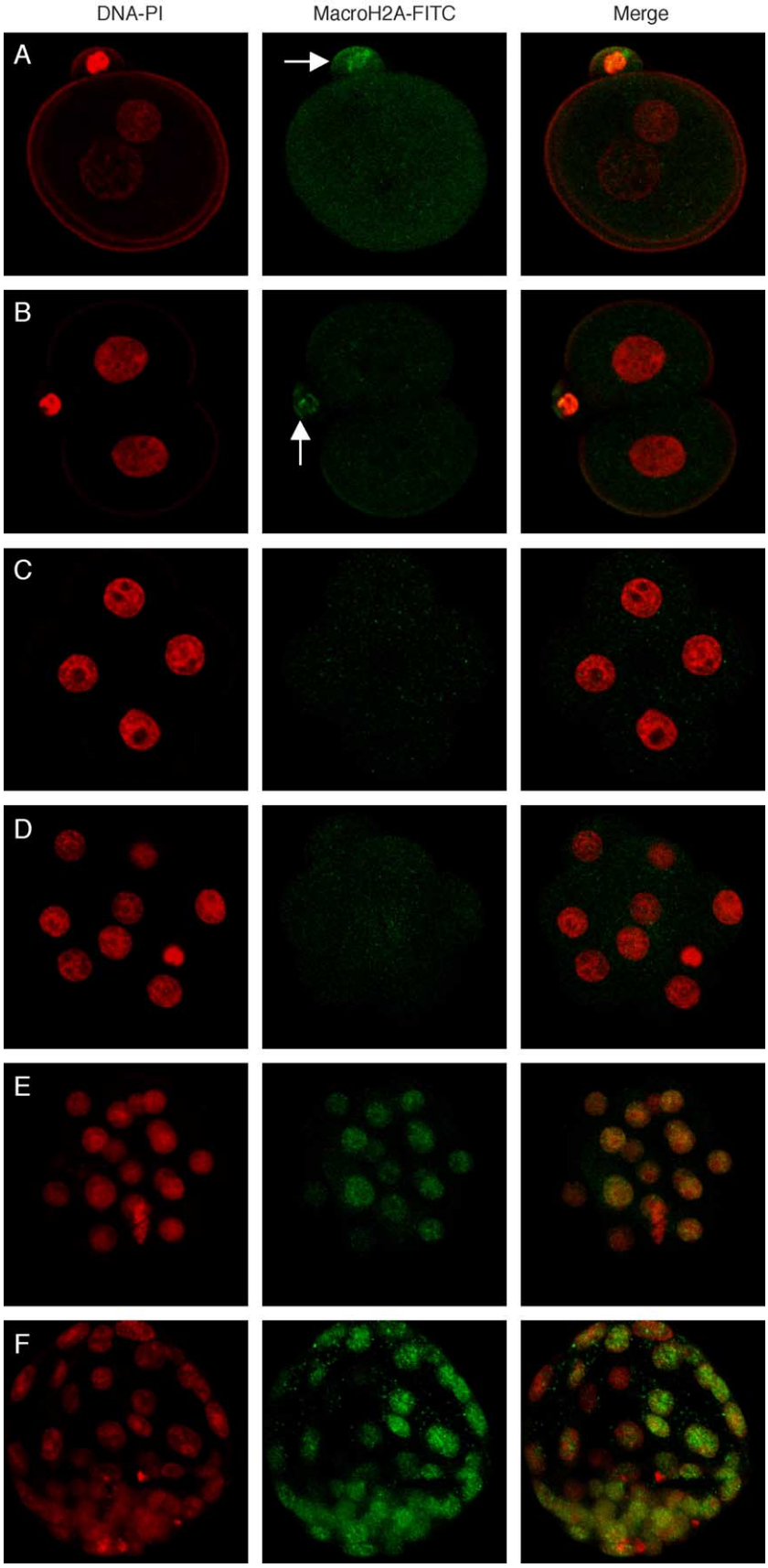
DNA-PI
MacroH2A-FITC
Merge
A
B
C
D
E
F

the contents into the TYH medium (Toyoda et al., 1971). Sperm were resuspended in TYH medium at a density of 5–10 million/ml, then incubated at 37°C, 5% CO_2, for 45 min prior to ICSI. The sperm suspension was then mixed with an equal volume of 12% (w/v) polyvinyl pyrolidone (PVP; Mr 360 × 10^3) dissolved in saline (0.9% NaCl). Mature MII oocytes were collected from B6D2F1 female mice at 14 h after hCG treatment and transferred into M2 medium before injection. Holding pipettes with 80 μm outside and 15 μm inside diameters were created using a pipette puller (P-87; Sutter Instrument Co., Novato, CA). Injection pipettes (6–8 μm inside diameter) were loaded with mercury and attached to a piezo-driving unit (PMAS-CT150, Prime Tech, Japan). Each sperm head was cut off using piezo pulses in conjunction with the injection pipette. Sperm heads were then washed and injected into the oocytes after piezo drilling through the zona and oolemma. The procedure of micromanipulation was essentially as described (Kimura and Yanagimachi, 1995), except that it was done at room temperature (20–24°C). After ICSI, injected oocytes were fixed after 15 min, 1, 3, 5, and 7 h of KSOM + AA medium incubation at 37°C, 5% CO_2.

Immunofluorescence and laser-scanning confocal microscopy

The rabbit anti-macroH2A antibody used in this study was created by inoculating a rabbit with the recombinant nonhistone domain (NHD) obtained by expression of an NHD fragment of a macroH2A1.2 cDNA fused to a GST expression vector. Precise details concerning the creation of this antibody are presented in a separate manuscript (Ma et al., submitted for publication). This antibody recognizes a single 42-kDa band (macroH2A) on Western blots of mouse protein and identifies inactive X chromosomes in female somatic cells (Akbarian et al., 2001; Ganesan et al., 2002; Wutz et al., 2002).

Oocytes and embryos were prepared for immunofluorescence by fixation in a 4% paraformaldehyde solution at room temperature for 15 min. They were then washed in phosphate-buffered saline (PBS) with 0.2% Tween 20 three times, and left in blocking buffer (PBS/0.2% Tween 20 and 10 mg/ml BSA) for 30 min at 37°C. Oocytes and embryos were then double stained to visualize macroH2A and DNA. Briefly, samples were incubated in rabbit anti-histone macroH2A antibody (Ma et al., submitted for publication) diluted 1:1000 for 30 min at 37°C. Embryos were then washed in PBS/0.2% Tween 20 three times and incubated in fluorescein isothiocyanate (FITC)-conjugated donkey anti-rabbit IgG (cat. no. 711-095-152, Jackson ImmunoResearch Inc., West Grove, PA) (1:200) for 1 h at 37°C. Finally, oocytes or embryos were washed three times in PBS/0.2% Tween 20, stained for DNA with 2.5 μg/ml propidium iodide, and mounted in PBS containing 50% glycerol and 25 mg/ml NaN_3. Oocytes and embryos were analyzed with a laser-scanning confocal microscope (Leica TCS SP2, Mannheim, Germany). Individual confocal sections were electronically merged so that all nuclei were visible in a single image. For antibody penetration controls (Fig. 5), embryos were processed as above and doubly stained for macroH2A (detected with goat anti-rabbit IgG conjugated to rhodamine Red-X (cat. no. 111-295-144, Jackson ImmunoResearch Inc.) (1:200) for 1 h at 37°C. and a mouse monoclonal pan-histone antibody (Chemicon, cat. no. MAB052) (1:100) [detected with goat anti-mouse IgG conjugated to FITC (cat. no. 115-095-160), Jackson ImmunoResearch Inc.] (1:200) for 1 h at 37°C.

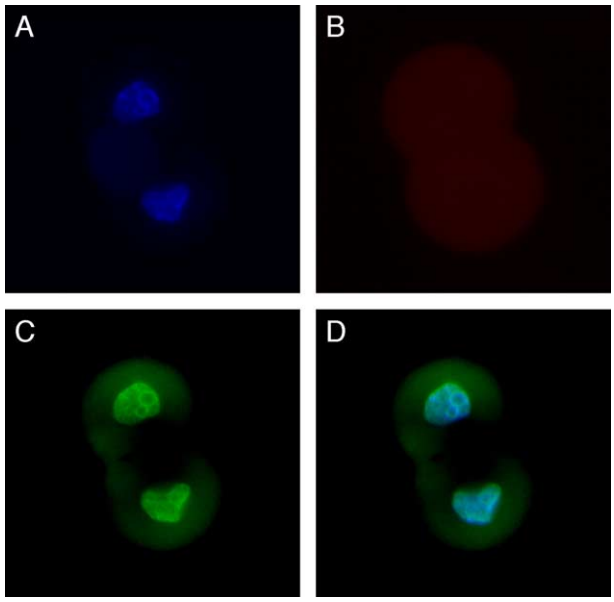

Fig. 5. Antibody penetration control. A representative 2-cell embryo is shown that was stained with (A) DAPI to visualize DNA, (B) α-macroH2A antibody detected with rhodamine Red-X, and (C) a mouse pan-histone antibody detected with FITC. A three-color merge is shown in panel D. These results indicate that chromatin can be readily detected in embryos during developmental stages that lack macroH2A.

Reagents used for additional immunofluorescence analyses follow. Double antibody staining was performed with a pan-histone antibody (Chemicon, cat. no. MAB052 diluted 1:100) and goat polyclonal HP1β (Abcam, cat. no. 11164, diluted 1:50). In addition, anti-γ-tubulin (Sigma, cat. no. T-6557, diluted 1:50), and human anti-centromere proteins (CREST) (Antibodies Incorporated, cat. no. 15-235, diluted 1:40), were used in combination with anti-macroH2A (1:1000). Rabbit primary antibodies were detected with FITC- or TRITC-conjugated anti-rabbit IgG (cat. no. 711-

Fig. 4. Distribution of macroH2A during mouse preimplantation embryonic development. Staged preimplantation embryos were stained with propidium iodide to visualize the DNA (DNA-PI) combined with immunodetection with α-macroH2A antibody detected with FITC (MacroH2A-FITC). (A) Representative zygote with 2 pronuclei. (B) Representative 2-cell embryo (arrows in rows A and B indicate macroH2A content in residual polar bodies). (C) 4-cell embryo. (D) 8-cell embryo. (E) Representative morula. (F) Representative blastocyst.

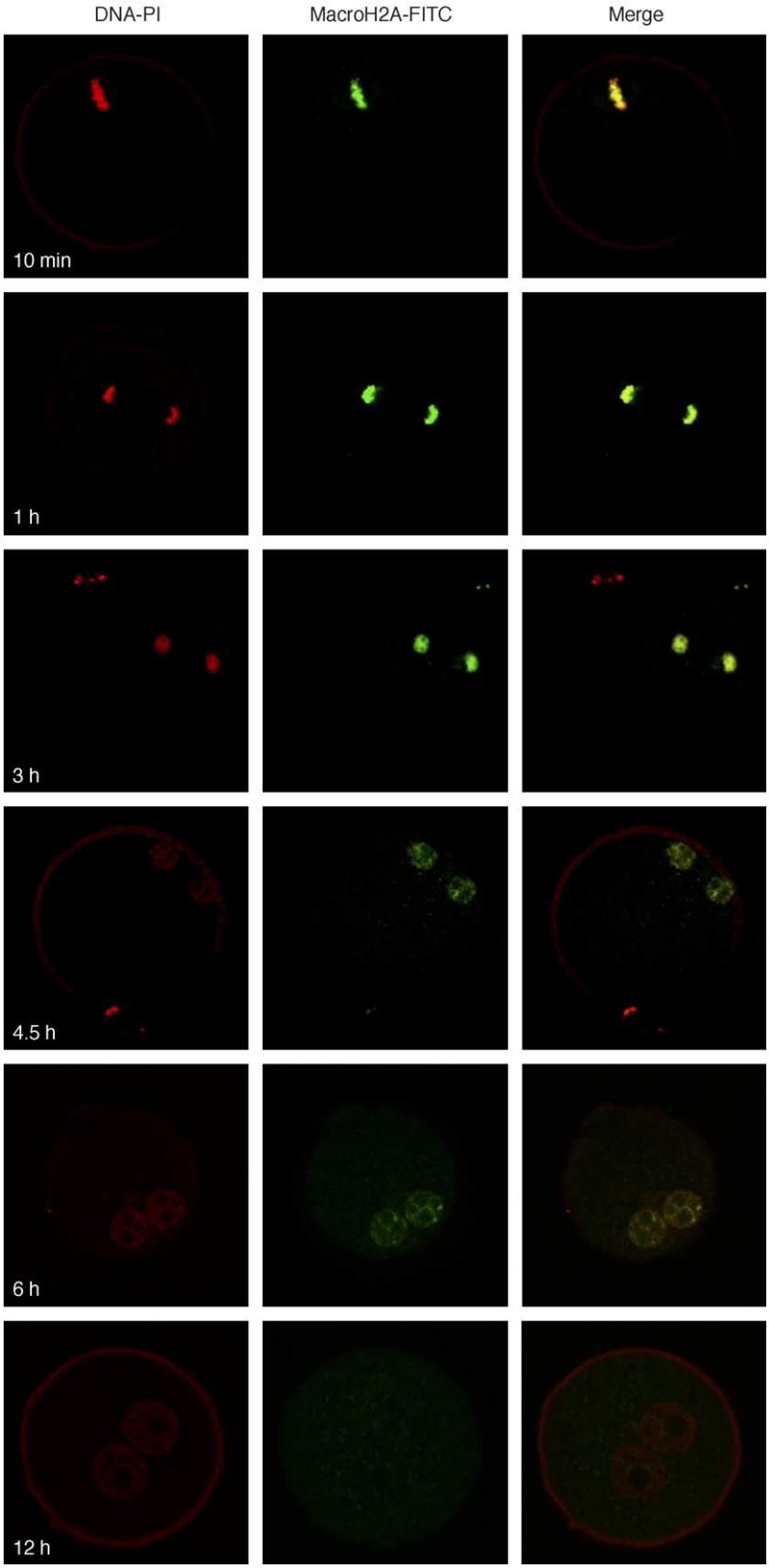
DNA-PI
MacroH2A-FITC
Merge
10 min
1 h
3 h
4.5 h
6 h
12 h

095-152 and cat. no. 711-025-152, Jackson ImmunoResearch Laboratories, 1:200). Mouse pan-histone or γ-tubulin antibodies were detected with donkey anti-mouse TRITC-conjugated IgG (cat. no. 715-025-150, Jackson ImmunoResearch Inc., 1:200). The HP1β antibodies were detected with donkey anti-goat FITC-conjugated IgG (cat. no. 705-095-003, Jackson ImmunoResearch Inc., 1:200), and CREST antibodies were detected with goat anti-human TRITC-conjugated IgG (cat. no. 109-025-003, Jackson ImmunoResearch Inc., 1:200). As before, oocytes were mounted in PBS containing 50% glycerol and 25 mg/ml NaN_3 as an antifading reagent and analyzed with a laser-scanning confocal microscope (Leica TCS SP2, Mannheim, Germany).

Results

MacroH2A distribution in developing and mature oocytes

We investigated the distribution of macroH2A during the course of the mouse oocyte maturation process. To do this, we collected granulosa oocyte complexes (GOCs) from ovaries and assessed oocytes stages. Oocytes containing germinal vesicles at the late growth (lg-GV) stage were surrounded by compact masses of granulosa cells and had oocyte diameters of less than 70 μm. Oocytes containing fully grown germinal vesicles (fg-GV) had diameters greater than 75 μm and loosely attached granulosa cells. Both lg-GV and fg-GV oocytes contained macroH2A signal that colocalized with condensed chromatin (Figs. 1A and B). However, macroH2A exhibited more intense deposition in lg-GV oocytes, where it was highly concentrated in several discrete spots (Fig. 1A). Of 35 GV stage oocytes, all had readily detectable macroH2A present in the nucleus (Table 1). A portion of the total macroH2A pool was present in an extranuclear position likely coincident with centrosomes, a localization pattern for macroH2A previously observed in embryonic stem cells and certain somatic cells (Chadwick and Willard, 2002; Mermoud et al., 2001; Rasmussen et al., 2000). In mature MII oocytes, macroH2A still associated with chromosomes, which had aligned on the metaphase II plate (Fig. 1C). Of 17 MII stage oocytes, all had macroH2A present upon chromosomes aligned at the metaphase plate (Table 1).

We performed double immunofluorescence experiments to more fully investigate the distribution of macroH2A relative to oocyte chromatin. Analysis of macroH2A distribution as compared to total chromatin (using a pan-histone antibody) revealed that macroH2A was spatially restricted to highly condensed subregions of chromatin in lg-GV and fg-GV oocytes (Fig. 2A). Because this pattern was reminiscent of pericentric heterochromatin, we co-stained for macroH2A and heterochromatin protein 1-β (HP1β), a known component of pericentric heterochromatin (Fig. 2B) (Furuta et al., 1997; Motzkus et al., 1999; Wreggett et al., 1994). We observed a high degree of colocalization between macroH2A and HP1β (Fig. 2B).

We next sought to investigate the small extranuclear concentrations of macroH2A in developing oocytes. We observed that extranuclear macroH2A colocalizes with γ-tubulin (a centrosomal marker) in lg-GV oocytes (Fig. 3A). In addition, we found that some macroH2A and γ-tubulin was concentrated as spindle poles in MII oocytes (Fig. 3B). Though similar in size, punctate concentrations of macroH2A within the nuclear volume colocalized with interphase centromere proteins visualized with CREST antisera (human scleroderma autoimmune serum that detects centromeric kinetochore proteins).

Together, these results indicate that a maternal store of macroH2A exists in developing and mature oocytes, where the majority of macroH2A resides in pericentric heterochromatin (as judged by its proximity to HP1β and kinetochore proteins). In addition, a small pool of macroH2A associates with centrosomes, a localization pattern previously described in other cells (Chadwick and Willard, 2002; Mermoud et al., 2001; Rasmussen et al., 2000).

MacroH2A in preimplantation embryos

Because a maternal store of macroH2A resides at the metaphase plate in mature oocytes, we investigated the fate of this store in preimplantation embryos. We examined zygotes, 2-, 4-, 8-, and 9- to 12-cell embryos, morula, and blastocysts for the distribution of macroH2A protein. Surprisingly, we found that macroH2A was undetectable in normal embryos by the late 2 pronuclei (late 2PN) stage (Fig. 4A). We also found that macroH2A was undetectable in the cells of 2-, 4-, and 8-cell embryos (Figs. 4B–D; Table 1). Though nuclear macroH2A was apparently absent in these early cleavage stage embryos, we often observed macroH2A protein in residual polar bodies (Fig. 4B), which served as internal controls for the detection of macroH2A by immunofluorescence. All embryos at morula and blastocyst stages contained nuclear macroH2A in blastomere nuclei (Figs. 4E and F; Table 1). After the appearance of macroH2A of embryonic origin, the intensity of nuclear macroH2A immunostaining gradually increased until embryos reached the blastocyst stage (Fig. 4F), where macroH2A was observed in all nuclei of the inner cell mass and trophectoderm, a result consistent with a previous report (Costanzi et al., 2000).

Because early preimplantation embryos contain relatively large volumes of cytoplasm and nucleoplasm, we performed

Fig. 6. Localization of macroH2A in parthenogenetic activated oocytes. Unfertilized MII oocytes were activated with strontium and fixed for immunostaining at 10 min, 1, 3, 4.5, 6, and 12 h after activation. Activated oocytes were stained with propidium iodide to detect DNA (DNA-PI) and macroH2A was detected by immunofluorescence (macroH2A-FITC). MacroH2A was associated with DNA on the initial meiotic metaphase plate and during pronuclear decondensation though the signal is successively lost during the decondensation process prior to synkaryogamy.

control experiments to insure that antibodies can effectively penetrate to chromatin. We subjected early embryos to double immunofluorescence designed to simultaneously detect macroH2A and histones using a monoclonal pan-histone antibody that recognizes the histone fold motif (Chemicon, cat. no. MAB052). We found that bulk histones but not macroH2A could be readily identified in early preimplantation embryos (Fig. 5). We conclude that macroH2A is rapidly lost from embryos by the late 2PN stage and that nuclear macroH2A of embryonic origin does not appear until after the

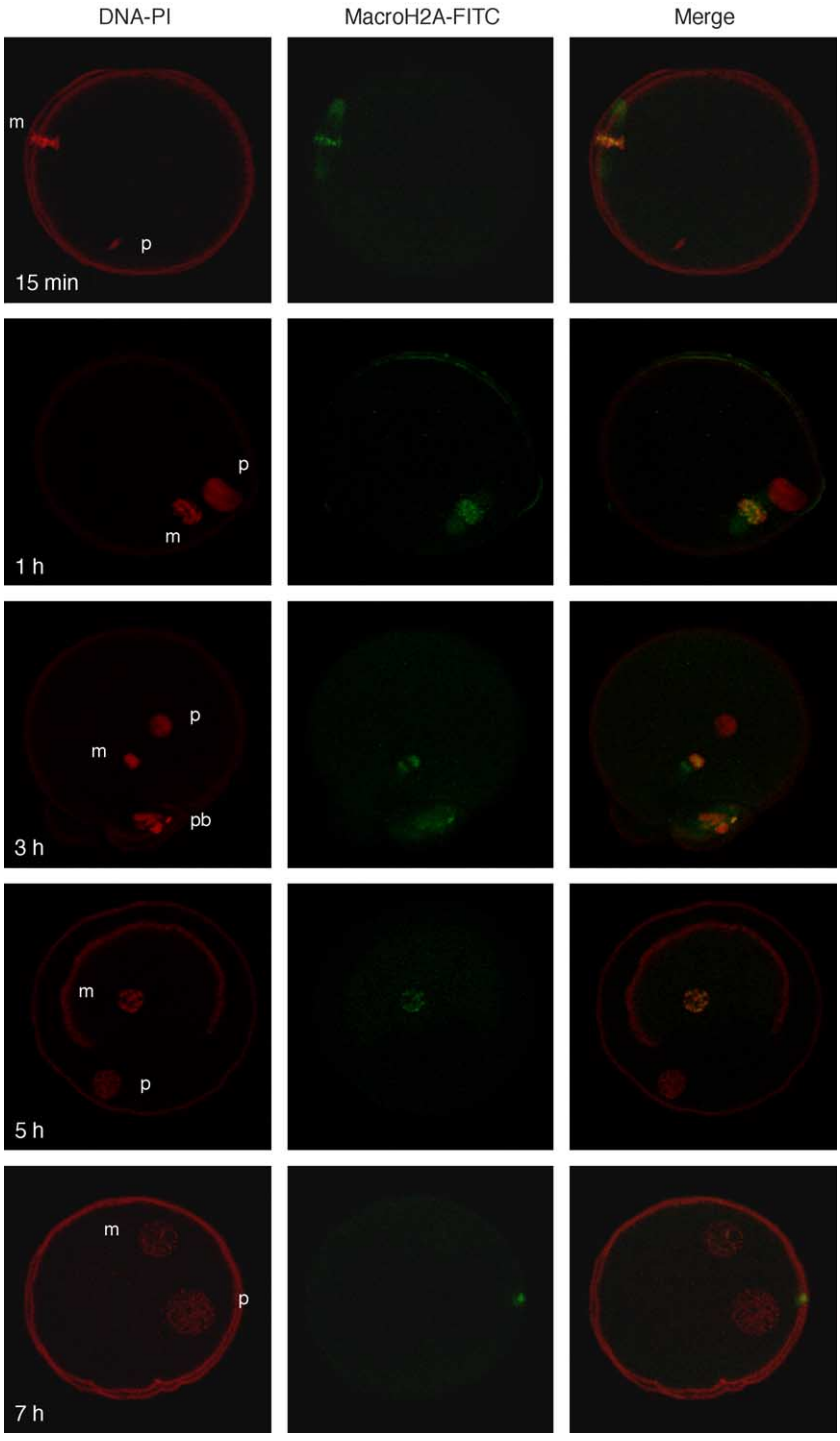

Fig. 7. Localization of macroH2A in ICSI embryos. Unfertilized MII oocytes were injected with single sperm heads, then fixed for immunostaining at 15 min, 1, 3, 5, and 7 h after injection. Embryos derived by ICSI were stained with propidium iodide to detect DNA (DNA-PI) and macroH2A was detected by immunofluorescence (macroH2A-FITC). MacroH2A was associated with maternal chromosomes initially present at the meiotic metaphase plate but was progressively lost from the decondensing female pronuclei (m). In contrast, macroH2A was undetectable on paternal pronuclei (p) throughout the decondensation process. This maternal/paternal asymmetry persisted until macroH2A became undetectable at 7 h post-ICSI.

8-cell stage. Hence, cleavage stage embryos execute their first three to four mitotic divisions in the absence of detectable macroH2A protein.

At the 70 h time point, we observed mostly 8-cell embryos, all of which lacked detectable macroH2A in blastomeres (Table 1). However, a few 70-h embryos had undergone subsequent asynchronous cell divisions resulting in embryos with 9–12 cells ("9–12 cell" embryos; Table 1). We observed the earliest appearance of macroH2A of embryonic origin in these post-8-cell embryos. Four post-8-cell embryos exhibited extranuclear accumulations of macroH2A near the cytoplasmic membrane, possibly representing newly synthesized macroH2A, while three 9- to 12-cell embryos had barely detectable macroH2A present in the nucleus (Table 1). We conclude that the onset of embryonic macroH2A expression commences immediately following the 8-cell stage.

MacroH2A in parthenogenetic embryos

We investigated the behavior of macroH2A in parthenogenetically activated oocytes to more closely follow the loss of macroH2A from pronuclei. Mature MII oocytes were collected from mouse oviducts and activated to undergo cell division through the use of strontium and cytochalasin B. Activated oocytes were fixed for immunofluorescence after 10 min, 1, 3, 4.5, 6, and 12 h (Fig. 6). After 10 min of activation, chromosomes (containing maternal macroH2A) still resided on the metaphase plate. After 1 h, we observed an anaphase configuration of chromosomes, which still possessed macroH2A. By 3 h, condensed pronuclei had formed, which still contained abundant macroH2A. Pronuclei underwent a progressive decondensation at 4.5 and 6 h time points, associated with increasingly diffuse macroH2A immunostaining. After 12 h of development, parthenogenetic embryos lacked detectable macroH2A.

MacroH2A associates exclusively with maternal pronuclei prior synkaryogamy

The previous parthenogenesis results confirmed that macroH2A is gradually lost from female pronuclei after oocyte activation. To more precisely investigate the behavior of macroH2A in normal embryos created by fertilization, we performed intracytoplasmic sperm injection (ICSI) to generate temporally synchronized cohorts of embryos. Following injection of sperm heads into mature MII oocytes, zygotes were fixed for immunofluorescence after 15 min, 1, 3, 5, and 7 h (Fig. 7; Table 2). At 15 min post-ICSI, maternal chromosomes (containing macroH2A) still resided on metaphase plates, while injected sperm heads were condensed and devoid of detectable macroH2A. After 1 h, paternal genome decondensation was well under way, but paternal pronuclei lacked detectable macroH2A. In contrast, the maternal chromosomes were entering meiotic anaphase after 1 h, with abundant macroH2A still present upon maternal chromosomes. By 3 h, decondensed paternal pronuclei were extensively decondensed and devoid of detectable macroH2A, while maternal macroH2A was distributed between decondensed female pronuclei and polar bodies. This asymmetry in macroH2A localization persisted into the 5-h time point, but by 7 h macroH2A became undetectable.

Table 2
Asymmetric distribution of macroH2A in parental genomes following fertilization by ICSI

Time after ICSI	Number examined	No. of embryos showing macroH2A in paternal pronucleus (%)	No. of embryos showing macroH2A signal in maternal pronucleus (%)
15 min	6	0 (0)	6 (100)
1 h	5	0 (0)	5 (100)
3 h	6	0 (0)	6 (100)
5 h	4	0 (0)	4 (100)
7 h	5	0 (0)	0 (0)

Discussion

These results describe for the first time the kinetics of macroH2A expression and localization during the complete course of oocyte maturation and preimplantation development. The results indicate that the expression and localization of macroH2A are carefully orchestrated and that a maternal store of macroH2A is rapidly removed after fertilization, a process that is complete by the late 2PN stage. Embryos then execute three cell cycles with undetectable levels of macroH2A prior to the appearance of macroH2A of embryonic origin.

Mature oocytes are transcriptionally inactive and contain abundant macroH2A present at the metaphase plate. In late 2PN embryos, we find macroH2A only within residual polar bodies, which likely represents macroH2A of maternal origin that is extruded with polar bodies. We followed the loss of macroH2A from female pronuclei by activating oocytes to undergo parthenogenetic development. We found that parthenogenetic pronuclei progressively lose macroH2A as they decondense, but we cannot at present determine if loss of macroH2A is an active process or a passive event caused by a failure to reassemble macroH2A chromatin during the first embryonic S-phase. Our experiments with ICSI revealed that a maternal–paternal asymmetry exists during the initial hours after fertilization in which macroH2A is preferentially associated with female pronuclei. This sequence is similar to that described for methylation of lysine 9 of histone H3, which also shows a transient maternal preference shortly after fertilization (Liu et al., 2004). These issues aside, it is clear that late 2PN embryos derived by normal fertilization, parthenogenesis, or ICSI lack appreciable amounts of macroH2A.

Previous studies involving macroH2A proteins have been complicated by the existence of at least three related macroH2A protein isoforms. In mice, the gene encoding macroH2A1 yields two alternatively spliced transcripts resulting in two protein isoforms of similar molecular weight, macroH2A1.1 and macroH2A1.2 (Pehrson et al., 1997; Rasmussen et al., 1999). The antibody used in this study (Ma et al., submitted for publication) was generated by inoculating rabbits with a recombinant protein corresponding to the entire nonhistone domain of macroH2A1.2. Therefore, this antibody does not likely distinguish between macroH2A1.1/1.2 protein isoforms. Additional studies will be required to assess subtle differences (if any) in the distribution of specific macroH2A protein isoforms in oocytes and preimplantation embryos. A second gene encodes a related protein, macroH2A2, that differs substantially from the macroH2A1.1/1.2 isoforms (Chadwick and Willard, 2001; Costanzi and Pehrson, 2001). Analyses of human cells that express both macroH2A1 and macroH2A2 proteins revealed that similar but not identical subnuclear localization patterns exist for these proteins (Costanzi and Pehrson, 2001), and that macroH2A2, like macroH2A1, can colocalize with inactive X chromosomes (Chadwick and Willard, 2001). Additional studies will be needed to determine if macroH2A2 is expressed in oocytes and preimplantation embryos.

Previous studies found macroH2A present at centrosomes in embryonic stem cells and a variety of somatic cells (Mermoud et al., 2001; Rasmussen et al., 2000). This centrosomal pool of macroH2A may represent material targeted for proteasome-dependent degradation, a mechanism common to a variety of other chromatin proteins (Chadwick and Willard, 2002). Further studies will be required to determine if 2PN embryos utilize this process for the degradation of macroH2A.

Chromatin is exquisitely and dynamically regulated in oocytes and early embryos as judged by a compilation of results from several studies. By comparing the kinetics of appearance and disappearance of chromatin markers for transcriptional activity and silence an interesting picture emerges (Fig. 8) in which broad reorganizations of chromatin are tightly orchestrated with the transcriptional status of the developing oocyte and embryonic genome. Acetylation events involving lysines 9 and 14 of histone H3 and lysines 5, 8, 12, and 16 of histone H4, have been carefully analyzed in maturing oocytes and preimplantation embryos. In all cases, acetylation was abundant in GV oocytes but severely reduced, if not absent, in transcriptionally quiescent MII oocytes (Kim et al., 2003). The mouse zygotic genome first becomes transcriptionally active in late 2PN embryos after the first zygotic S-phase (Ram and Schultz, 1993). Recent findings show that zygotic genome activation (ZGA) at the 2PN corresponds to the first of two waves of genome activation in preimplantation embryos (Hamatani et al., 2004). This initial wave of ZGA occurs as histones H3 and H4 become reacetylated (Kim et

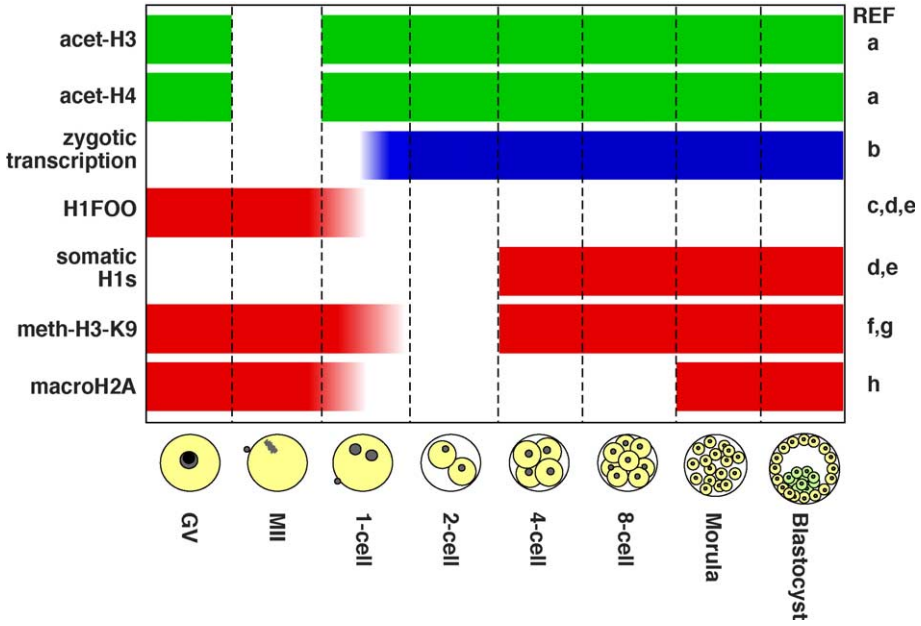

Fig. 8. Kinetics of chromatin assembly in maturing mouse oocytes and preimplantation embryos. Analysis of scientific literature reveals that transcriptionally permissive acetylation modifications (green bars) on histone H3 at lysines K9 and K14, and histone H4 at lysines K5, K8, K12, and K16, are absent in MII oocytes but reappear in 1-cell embryos prior to the onset of zygotic genome activation at the late 2PN stage (blue bar). Histone modifications and histone variants implicated in gene silencing (red bars) exhibit delayed kinetics. Maternal linker histone H1FOO is removed from late 2PN (1-cell) embryos and later replaced by somatic H1 linker histones. The transcriptionally repressive methyl-H3-K9 modification exhibits similar kinetics. Finally, macroH2A kinetics are shown, which are reminiscent of the H1FOO-somatic H1 histone transition. Note that repressive chromatin is assembled later than permissive chromatin and after zygotic genome activation. References: a: Kim et al. (2003); b: Ram and Schultz (1993); c: Tanaka et al. (2001); d: Gao et al. (2004); e: Teranishi et al. (2004); f: Arney et al. (2002); g: Liu et al. (2004); h: this study.

al., 2003). These findings agree with a previous study using antibodies to acetyl H4-K5 and a pan-acetylated histone antibody (Adenot et al., 1997). A subsequent (and more substantial) wave of embryonic genome transcription occurs just prior to compaction and morula formation (Hamatani et al., 2004).

In contrast, the establishment of repressive chromatin occurs well after ZGA and relies heavily upon replacement events involving histone variants. During ovarian development, somatic linker H1 histones are progressively lost from developing oocytes (Clarke et al., 1997). The oocyte-specific linker histone H1FOO (H1oo) (Tanaka et al., 2001) becomes present in the chromatin of GV and MII oocytes and is rapidly incorporated into male pronuclei shortly after fertilization (Gao et al., 2004). However, embryos lack significant levels of H1 histones at the 2-cell stage (Tanaka et al., 2001) prior to replacement with somatic H1s in the nuclei of 4-cell and later embryos (Gao et al., 2004; Teranishi et al., 2004). An oocyte-specific form of linker histone, H1FOO, is removed by the late 2PN stage but replaced with somatic H1s at the 4-cell stage (Gao et al., 2004). Our results show that macroH2A is not acquired in embryonic chromatin until after the 8-cell stage. Thus, early embryos do not acquire macroH2A until 1–2 cell divisions after the somatic H1 transition (Fig. 8). Histone H3 dimethylated at lysine 9 (me-H3-K9) is present in GV and mature oocytes but is absent from sperm and the male genome until the 4-cell stage. The me-H3-K9 modification persists on the maternal genome in both late 2PN and 2-cell embryos (Liu et al., 2004). The asymmetry of me-H3-K9 with regards to male and female pronuclei is associated with the preferential recruitment of the heterochromatin component HP1β to the maternal genome in the period immediately following fertilization (Arney et al., 2002). In similar fashion, we find that macroH2A preferentially associates with the maternal pronucleus in zygotes, prior to its loss before synkaryogamy. Thus, a striking asymmetry exists in zygote chromatin because maternal pronuclei retain patterns of histone methylation and macroH2A content that are undetectable in male pronuclei. This situation may have implications for epigenetic regulation of imprinting. HP1β (Arney et al., 2002) is recruited to the paternal genome in late 2PN embryos, prior to the onset of paternal H3-K9 methylation, a surprising result since methylation of H3-K9 can serve as a *cis*-acting binding site for HP1s (Lachner et al., 2001; Maison et al., 2002; Rea et al., 2000). In contrast, HP1γ is uniformly recruited to both male and female pronuclei at the late 2PN stage (Arney et al., 2002).

The regulation of gene expression during the remainder of development involves numerous lineage-specific gene-silencing events involving macroH2A and many other heterochromatin proteins. We find it interesting macroH2A of embryonic origin is not associated with the embryonic genome until well after acetylation of genomic core histones H3 and H4 has occurred at the 2PN stage (Kim et al., 2003). Indeed, embryonic macroH2A is not present until after both waves of embryonic genome activation have been initiated (Hamatani et al., 2004). Taken together, these results suggest a possible sequence of gene regulation in which the zygotic genome is first widely activated, perhaps in an unregulated fashion. Subsequent gene-silencing events may represent the first instance of regulated gene expression in the embryo.

Acknowledgments

We thank Therese Doherty for proofreading of this manuscript. This work was supported in part by the Robert Leet and Clara Guthrie Patterson Trust.

References

Adenot, P.G., Mercier, Y., Renard, J.P., Thompson, E.M., 1997. Differential H4 acetylation of paternal and maternal chromatin precedes DNA replication and differential transcriptional activity in pronuclei of 1-cell mouse embryos. Development 124, 4615–4625.

Akbarian, S., Chen, R.Z., Gribnau, J., Rasmussen, T.P., Fong, H., Jaenisch, R., Jones, E.G., 2001. Expression pattern of the Rett syndrome gene MeCP2 in primate prefrontal cortex. Neurobiol. Dis. 8, 784–791.

Angelov, D., Molla, A., Perche, P.Y., Hans, F., Cote, J., Khochbin, S., Bouvet, P., Dimitrov, S., 2003. The histone variant macroH2A interferes with transcription factor binding and SWI/SNF nucleosome remodeling. Mol. Cell 11, 1033–1041.

Arney, K.L., Bao, S., Bannister, A.J., Kouzarides, T., Surani, M.A., 2002. Histone methylation defines epigenetic asymmetry in the mouse zygote. Int. J. Dev. Biol. 46, 317–320.

Chadwick, B.P., Willard, H.F., 2001. Histone H2A variants and the inactive X chromosome: identification of a second macroH2A variant. Hum. Mol. Genet. 10, 1101–1113.

Chadwick, B.P., Willard, H.F., 2002. Cell cycle-dependent localization of macroH2A in chromatin of the inactive X chromosome. J. Cell Biol. 157, 1113–1123.

Clarke, H.J., Bustin, M., Oblin, C., 1997. Chromatin modifications during oogenesis in the mouse: removal of somatic subtypes of histone H1 from oocyte chromatin occurs post-natally through a post-transcriptional mechanism. J. Cell Sci. 110 (Pt. 4), 477–487.

Costanzi, C., Pehrson, J.R., 1998. Histone macroH2A1 is concentrated in the inactive X chromosome of female mammals. Nature 393, 599–601.

Costanzi, C., Pehrson, J.R., 2001. MACROH2A2, a new member of the MARCOH2A core histone family. J. Biol. Chem. 276, 21776–21784.

Costanzi, C., Stein, P., Worrad, D.M., Schultz, R.M., Pehrson, J.R., 2000. Histone macroH2A1 is concentrated in the inactive X chromosome of female preimplantation mouse embryos. Development 127, 2283–2289.

Furuta, K., Chan, E.K., Kiyosawa, K., Reimer, G., Luderschmidt, C., Tan, E.M., 1997. Heterochromatin protein HP1Hsbeta (p25beta) and its localization with centromeres in mitosis. Chromosoma 106, 11–19.

Ganesan, S., Silver, D.P., Greenberg, R.A., Avni, D., Drapkin, R., Miron, A., Mok, S.C., Randrianarison, V., Brodie, S., Salstrom, J., Rasmussen, T.P., Klimke, A., Marrese, C., Marahrens, Y., Deng, C.X., Feunteun, J., Livingston, D.M., 2002. BRCA1 supports XIST RNA concentration on the inactive X chromosome. Cell 111, 393–405.

Gao, S., Chung, Y.G., Parseghian, M.H., King, G.J., Adashi, E.Y., Latham, K.E., 2004. Rapid H1 linker histone transitions following fertilization or somatic cell nuclear transfer: evidence for a uniform developmental program in mice. Dev. Biol. 266, 62–75.

Hamatani, T., Carter, M.G., Sharov, A.A., Ko, M.S., 2004. Dynamics of global gene expression changes during mouse preimplantation development. Dev. Cell 6, 117–131.

Hogan, B., Beddington, R., Costantini, F., Lacy, E., 1994. Manipulating the Mouse Embryo. A Laboratory Manual. Cold Spring Harbor Laboratory Press, Cold Spring Harbor, NY.

Hoyer-Fender, S., Costanzi, C., Pehrson, J.R., 2000. Histone macroH2A1.2 is concentrated in the XY-body by the early pachytene stage of spermatogenesis. Exp. Cell Res. 258, 254–260.

Hoyer-Fender, S., Czirr, E., Radde, R., Turner, J.M., Mahadevaiah, S.K., Pehrson, J.R., Burgoyne, P.S., 2004. Localisation of histone macroH2A1.2 to the XY-body is not a response to the presence of asynapsed chromosome axes. J. Cell Sci. 117, 189–198.

Kim, J.M., Liu, H., Tazaki, M., Nagata, M., Aoki, F., 2003. Changes in histone acetylation during mouse oocyte meiosis. J. Cell Biol. 162, 37–46.

Kimura, Y., Yanagimachi, R., 1995. Mouse oocytes injected with testicular spermatozoa or round spermatids can develop into normal offspring. Development 121, 2397–2405.

Lachner, M., O'Carroll, D., Rea, S., Mechtler, K., Jenuwein, T., 2001. Methylation of histone H3 lysine 9 creates a binding site for HP1 proteins. Nature 410, 116–120.

Ladurner, A.G., 2003. Inactivating chromosomes: a macro domain that minimizes transcription. Mol. Cell 12, 1–3.

Liu, H., Kim, J.M., Aoki, F., 2004. Regulation of histone H3 lysine 9 methylation in oocytes and early pre-implantation embryos. Development 131, 2269–2280.

Ma, Y., Jackson-Grusby, L., Mastrangelo, M.A., Jacobs, S.B., Rasmussen, T.P., 2004. DNA CpG hypomethylation induces heterochromatin remodeling involving the histone variant macroH2A. (submitted for publication).

Maison, C., Bailly, D., Peters, A.H., Quivy, J.P., Roche, D., Taddei, A., Lachner, M., Jenuwein, T., Almouzni, G., 2002. Higher-order structure in pericentric heterochromatin involves a distinct pattern of histone modification and an RNA component. Nat. Genet. 30, 329–334.

Mayer, W., Niveleau, A., Walter, J., Fundele, R., Haaf, T., 2000. Demethylation of the zygotic paternal genome. Nature 403, 501–502.

Mermoud, J.E., Tassin, A.M., Pehrson, J.R., Brockdorff, N., 2001. Centrosomal association of histone macroH2A1.2 in embryonic stem cells and somatic cells. Exp. Cell Res. 268, 245–251.

Motzkus, D., Singh, P.B., Hoyer-Fender, S., 1999. M31, a murine homolog of *Drosophila* HP1, is concentrated in the XY body during spermatogenesis. Cytogenet. Cell Genet. 86, 83–88.

Oswald, J., Engemann, S., Lane, N., Mayer, W., Olek, A., Fundele, R., Dean, W., Reik, W., Walter, J., 2000. Active demethylation of the paternal genome in the mouse zygote. Curr. Biol. 10, 475–478.

Pehrson, J.R., Fried, V.A., 1992. MacroH2A, a core histone containing a large nonhistone region. Science 257, 1398–1400.

Pehrson, J.R., Costanzi, C., Dharia, C., 1997. Developmental and tissue expression patterns of histone macroH2A1 subtypes. J. Cell Biochem. 65, 107–113.

Ram, P.T., Schultz, R.M., 1993. Reporter gene expression in G2 of the 1-cell mouse embryo. Dev. Biol. 156, 552–556.

Rasmussen, T.P., Huang, T., Mastrangelo, M.A., Loring, J., Panning, B., Jaenisch, R., 1999. Messenger RNAs encoding mouse histone macroH2A1 isoforms are expressed at similar levels in male and female cells and result from alternative splicing. Nucleic Acids Res. 27, 3685–3689.

Rasmussen, T.P., Mastrangelo, M.A., Eden, A., Pehrson, J.R., Jaenisch, R., 2000. Dynamic relocalization of histone MacroH2A1 from centrosomes to inactive X chromosomes during X inactivation. J. Cell Biol. 150, 1189–1198.

Rea, S., Eisenhaber, F., O'Carroll, D., Strahl, B.D., Sun, Z.W., Schmid, M., Opravil, S., Mechtler, K., Ponting, C.P., Allis, C.D., Jenuwein, T., 2000. Regulation of chromatin structure by site-specific histone H3 methyltransferases. Nature 406, 593–599.

Richler, C., Dhara, S.K., Wahrman, J., 2000. Histone macroH2A1.2 is concentrated in the XY compartment of mammalian male meiotic nuclei. Cytogenet. Cell Genet. 89, 118–120.

Tanaka, M., Hennebold, J.D., Macfarlane, J., Adashi, E.Y., 2001. A mammalian oocyte-specific linker histone gene H1oo: homology with the genes for the oocyte-specific cleavage stage histone (cs-H1) of sea urchin and the B4/H1M histone of the frog. Development 128, 655–664.

Teranishi, T., Tanaka, M., Kimoto, S., Ono, Y., Miyakoshi, K., Kono, T., Yoshimura, Y., 2004. Rapid replacement of somatic linker histones with the oocyte-specific linker histone H1foo in nuclear transfer. Dev. Biol. 266, 76–86.

Toyoda, Y., Yokoyama, M., Hoshi, T., 1971. Studies on the fertilization of mouse eggs in vitro: I. In vitro fertilization of eggs by fresh epididymal spermatozoa. Jpn. J. Anim. Reprod. 16, 147–151.

Turner, J.M., Burgoyne, P.S., Singh, P.B., 2001. M31 and macroH2A1.2 colocalise at the pseudoautosomal region during mouse meiosis. J. Cell Sci. 114, 3367–3375.

Turner, J.M., Mahadevaiah, S.K., Elliott, D.J., Garchon, H.J., Pehrson, J.R., Jaenisch, R., Burgoyne, P.S., 2002. Meiotic sex chromosome inactivation in male mice with targeted disruptions of Xist. J. Cell Sci. 115, 4097–4105.

Wreggett, K.A., Hill, F., James, P.S., Hutchings, A., Butcher, G.W., Singh, P.B., 1994. A mammalian homologue of *Drosophila* heterochromatin protein 1 (HP1) is a component of constitutive heterochromatin. Cytogenet. Cell Genet. 66, 99–103.

Wutz, A., Rasmussen, T.P., Jaenisch, R., 2002. Chromosomal silencing and localization are mediated by different domains of Xist RNA. Nat. Genet. 30, 167–174.